

Application to heated granular gases

A FAST SPECTRAL METHOD FOR THE INELASTIC  
BOLTZMANN COLLISION OPERATOR

Zheng Ma

Purdue University

Joint work with Jingwei Hu

## A GAS OF “MARBLES”



## A GAS OF “MARBLES”

- Granular materials: powders, grains
- Geophysics: sand dunes, volcanic flows
- Astrophysics: large scale formation



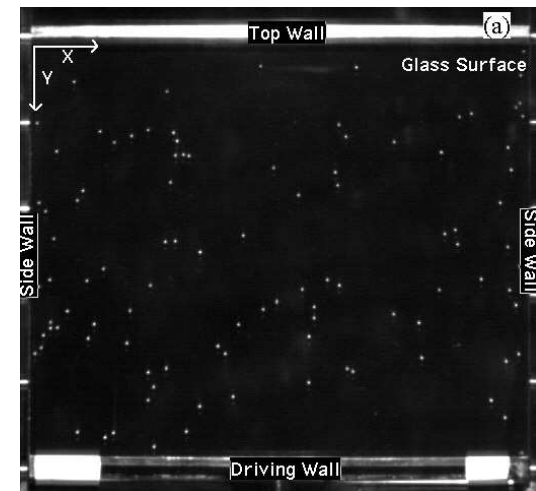
## GRANULAR GASES

- Collections of interacting discrete solid particles
- Under influence of gravity, particles can be fluidized by sufficiently strong forcing: vibration, shear or electric field
- Granular gas is also called “rapid granular flow”

# GRANULAR GASES VS. MOLECULAR GASES

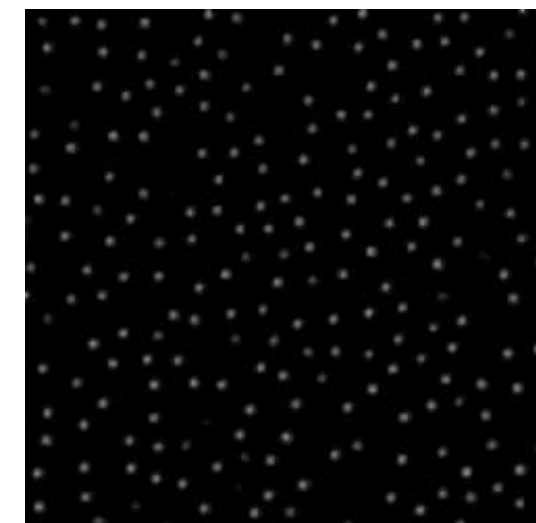
Characteristics:

- Hard sphere interactions
- Dissipative collisions



Main difference:

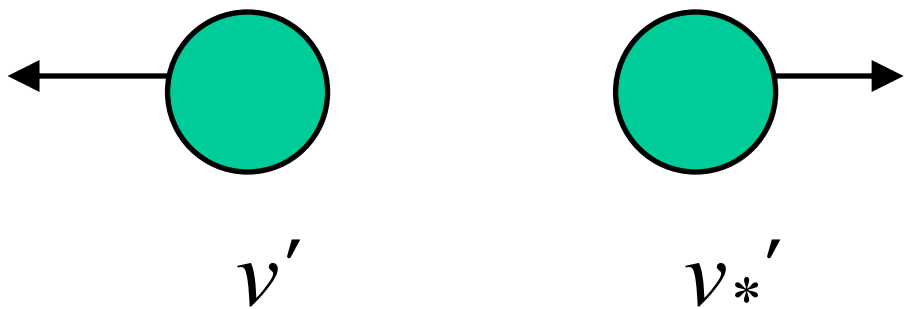
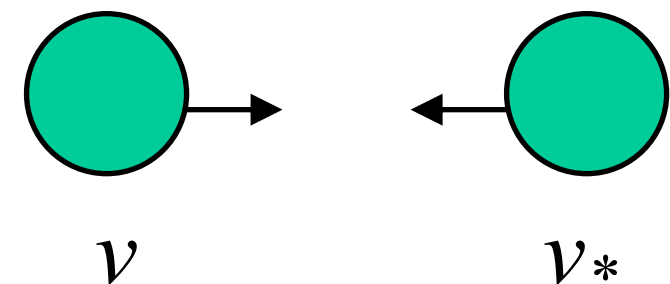
- Inelasticity of collisions
- Dissipation of energy



## INELASTIC COLLISIONS

$$(\nu' - \nu'_*) \cdot \omega = -e[(\nu - \nu_*) \cdot \omega], \quad 0 \leq e \leq 1.$$

$$\begin{cases} \nu' = \nu - \frac{1+e}{2}[(\nu - \nu_*) \cdot \omega]\omega, \\ \nu'_* = \nu_* + \frac{1+e}{2}[(\nu - \nu_*) \cdot \omega]\omega. \end{cases}$$



$$\nu' + \nu'_* = \nu + \nu_*; \quad |\nu'|^2 + |\nu'_*|^2 - |\nu|^2 - |\nu_*|^2 = -\frac{1-e^2}{2}[(\nu - \nu_*) \cdot \omega]^2 \leq 0.$$

## CHALLENGES

- Hydrodynamics: flow equations
- Kinetic theory: velocity statistics
- Sharp validity criteria are missing

## KINETIC THEORY

- Kinetic theory models the non-equilibrium dynamics of a gas (or any system comprised of a large number of particles)



- Applications: aerospace engineering, nuclear, plasma, radiological engineering condensed matter physics, biological and social sciences

## THE BOLTZMANN EQUATION

- A nonlinear phase space equation modeling particle transport and binary collisions
- It is the most fundamental equation in kinetic theory



## THE BOLTZMANN EQUATION

$$\partial_t f + \mathbf{v} \cdot \nabla f = Q[f],$$



- Spatially homogeneous and isotropic Boltzmann equation with a heating source

## COLLISION OPERATOR

Strong form:

$$\begin{aligned} Q(f, f)(v) &= \int_{\mathbb{R}^d} \int_{S^{d-1}} B_\omega(|\tilde{g}|, |\omega \cdot \hat{\tilde{g}}|) \tilde{f} \tilde{f}_* J \, d\omega \, dv_* - \int_{\mathbb{R}^d} \int_{S^{d-1}} B_\omega(|g|, |\omega \cdot \hat{g}|) f f_* \, d\omega \, dv_* \\ &:= Q^+(f, f) - Q^-(f, f), \end{aligned}$$

$\tilde{v}$  and  $\tilde{v}_*$  are pre-collisional velocities      $g := v - v_*$       $J = \left| \frac{\partial(\tilde{v}, \tilde{v}_*)}{\partial(v, v_*)} \right|$ .

$\tilde{v}$  and  $\tilde{v}_*$  do not coincide with  $v'$  and  $v'_*$  unlike the classical (elastic)

$B_\omega = B_\omega(|g|, |\omega \cdot \hat{g}|)$  is the collision kernel

## **COLLISION OPERATOR**

Weak forms:

$$\int_{\mathbb{R}^d} Q(f, f)(v) \varphi(v) \, dv = \int_{\mathbb{R}^d} \int_{\mathbb{R}^d} \int_{S^{d-1}} B_\omega(|g|, |\omega \cdot \hat{g}|) f f_* (\varphi' - \varphi) \, d\omega \, dv \, dv_*.$$

$$\int_{\mathbb{R}^d} Q(f, f)(v) \varphi(v) \, dv = \frac{1}{2} \int_{\mathbb{R}^d} \int_{\mathbb{R}^d} \int_{S^{d-1}} B_\omega(|g|, |\omega \cdot \hat{g}|) f f_* (\varphi' + \varphi'_* - \varphi - \varphi_*) \, d\omega \, dv \, dv_*.$$

$$\begin{cases} v' = \frac{v + v_*}{2} + \frac{1 - e}{4}(v - v_*) + \frac{1 + e}{4}|v - v_*|\sigma, \\ v'_* = \frac{v + v_*}{2} - \frac{1 - e}{4}(v - v_*) - \frac{1 + e}{4}|v - v_*|\sigma, \end{cases} \quad (g \cdot \omega)\omega = \frac{1}{2}(g - |g|\sigma).$$

## COLLISION OPERATOR

**Weak form 1:**

$$\int_{\mathbb{R}^d} Q(f, f)(v) \varphi(v) \, dv = \int_{\mathbb{R}^d} \int_{\mathbb{R}^d} \int_{S^{d-1}} B_\sigma(|g|, \sigma \cdot \hat{g}) f f_* (\varphi' - \varphi) \, d\sigma \, dv \, dv_*,$$

**Weak form 2:**

$$\int_{\mathbb{R}^d} Q(f, f)(v) \varphi(v) \, dv = \frac{1}{2} \int_{\mathbb{R}^d} \int_{\mathbb{R}^d} \int_{S^{d-1}} B_\sigma(|g|, \sigma \cdot \hat{g}) f f_* (\varphi' + \varphi'_* - \varphi - \varphi_*) \, d\sigma \, dv \, dv_*,$$

$$B_\sigma(|g|, \sigma \cdot \hat{g}) = C_\lambda |g|^\lambda, \quad 0 \leq \lambda \leq 1, \quad \text{variable hard sphere (VHS) model}$$

## INELASTIC BOLTZMANN WITH HEATING SOURCE

Moments and macroscopic quantities:

$$\rho = \int_{\mathbb{R}^d} f \, dv, \quad m = \int_{\mathbb{R}^d} fv \, dv, \quad E = \frac{1}{2} \int_{\mathbb{R}^d} f|v|^2 \, dv,$$

$$u = \frac{1}{\rho} \int_{\mathbb{R}^d} fv \, dv, \quad T = \frac{1}{d\rho} \int_{\mathbb{R}^d} f|v - u|^2 \, dv,$$

Conservation of mass and momentum:  $\rho \equiv \rho_0, \quad m \equiv m_0,$

$$\partial_t E - \varepsilon d\rho_0 = -\frac{1}{16} \int_{\mathbb{R}^d} \int_{\mathbb{R}^d} \int_{S^{d-1}} (1 - e^2) B_\sigma(|g|, \sigma \cdot \hat{g}) |g|^2 (1 - \sigma \cdot \hat{g}) f f_* \, d\sigma \, dv \, dv_*,$$

## MAXWELL MOLECULES

$$\begin{aligned}\partial_t E - \varepsilon d\rho_0 &= -\frac{1-e^2}{16} \int_{\mathbb{R}^d} \int_{\mathbb{R}^d} |g|^2 f f_* \, dv \, dv_* \\ &= -\frac{1-e^2}{16} \int_{\mathbb{R}^d} \int_{\mathbb{R}^d} (|v|^2 + |v_*|^2 - 2v \cdot v_*) f f_* \, dv \, dv_* \\ &= -\frac{1-e^2}{8} (2\rho_0 E - m_0^2).\end{aligned}$$

For simplicity, if we take the initial condition such that  $\rho_0 = 1$ ,  $u_0 = 0$ ,

$$\partial_t T - 2\varepsilon = -\frac{1-e^2}{4} T,$$

$$T = \left( T_0 - \frac{8\varepsilon}{1-e^2} \right) \exp\left(-\frac{1-e^2}{4} t\right) + \frac{8\varepsilon}{1-e^2}.$$

## NUMERICAL CHALLENGE

Major numerical difficulty: collision operator

- High dimensional integral
- Quadratic operator
- Need to capture high-order moments with good accuracy

## GENERAL STRATEGY

Probabilistic approach:

- DSMC: easy implementation, efficient, half-order accuracy, random fluctuations

Deterministic approach:

- Discrete velocity models: expensive, first or second order accuracy
- (Fourier) spectral method: relatively expensive, spectral accuracy

## FOURIER-GALERKIN SPECTRAL METHOD

Weak form:

$$\int_{\mathbb{R}^d} Q(f, f)(v) \varphi(v) \, dv = \int_{\mathbb{R}^d} \int_{\mathbb{R}^d} \int_{S^{d-1}} B_\sigma(|g|, \sigma \cdot \hat{g}) f(v) f(v - g) (\varphi(v') - \varphi(v)) \, d\sigma \, dg \, dv,$$

Assume  $f$  has a compact support:  $\text{Supp}_v(f) \approx B_S$

$$\int_{\mathbb{R}^d} Q(f, f)(v) \varphi(v) \, dv = \int_{\mathbb{R}^d} \int_{B_R} \int_{S^{d-1}} B_\sigma(|g|, \sigma \cdot \hat{g}) f(v) f(v - g) (\varphi(v') - \varphi(v)) \, d\sigma \, dg \, dv.$$

Fourier series:

$$f(v) \approx f_N(v) = \sum_{k=-\frac{N}{2}}^{\frac{N}{2}-1} \hat{f}_k e^{i \frac{\pi}{L} k \cdot v}, \quad \hat{f}_k = \frac{1}{(2L)^d} \int_{D_L} f(v) e^{-i \frac{\pi}{L} k \cdot v} \, dv.$$

## FOURIER-GALERKIN SPECTRAL METHOD

$$\begin{aligned}
\hat{Q}_k &:= \frac{1}{(2L)^d} \int_{D_L} Q(f_N, f_N)(v) e^{-i\frac{\pi}{L}k \cdot v} dv \\
&= \frac{1}{(2L)^d} \int_{D_L} \int_{B_R} \int_{S^{d-1}} B_\sigma(|g|, \sigma \cdot \hat{g}) f_N(v) f_N(v - g) \left( e^{-i\frac{\pi}{L}k \cdot v'} - e^{-i\frac{\pi}{L}k \cdot v} \right) d\sigma dg dv \\
&= \sum_{\substack{l,m=-\frac{N}{2} \\ l+m=k}}^{\frac{N}{2}-1} \int_{B_R} \int_{S^{d-1}} B_\sigma(|g|, \sigma \cdot \hat{g}) e^{-i\frac{\pi}{L}m \cdot g} \left( e^{i\frac{\pi}{L}\frac{1+e}{4}k \cdot (g - |g|\sigma)} - 1 \right) \hat{f}_l \hat{f}_m d\sigma dg,
\end{aligned}$$

Define the weight

$$G(l, m) = \int_{B_R} e^{-i\frac{\pi}{L}m \cdot g} \left[ \int_{S^{d-1}} B_\sigma(|g|, \sigma \cdot \hat{g}) \left( e^{i\frac{\pi}{L}\frac{1+e}{4}(l+m) \cdot (g - |g|\sigma)} - 1 \right) d\sigma \right] dg,$$

Then we get

$$\hat{Q}_k = \sum_{\substack{l,m=-\frac{N}{2} \\ l+m=k}}^{\frac{N}{2}-1} G(l, m) \hat{f}_l \hat{f}_m.$$

## FOURIER-GALERKIN SPECTRAL METHOD

- Precompute the weight: memory requirement  $O(N^{2d})$
- Online computation of weighted sum: complexity  $O(N^{2d})$

## A FAST SPECTRAL METHOD

- Main idea: use pure convolution instead of weighted sum
- Use FFT to perform the pure convolution

$$G(l, m) \approx \sum_{p=1}^{N_p} \alpha_p(l + m) \beta_p(m),$$
$$O(N_p N^d \log N)$$

$$\hat{Q}_k \approx \sum_{p=1}^{N_p} \alpha_p(k) \sum_{\substack{l, m = -\frac{N}{2} \\ l+m=k}}^{\frac{N}{2}-1} \hat{f}_l(\beta_p(m) \hat{f}_m),$$

## APPROXIMATE THE INTEGRAL

$$G(l, m) = \int_{B_R} e^{-i\frac{\pi}{L}m \cdot g} \left[ \int_{S^{d-1}} B_\sigma(|g|, \sigma \cdot \hat{g}) \left( e^{i\frac{\pi}{L}\frac{1+e}{4}(l+m) \cdot (g - |g|\sigma)} - 1 \right) d\sigma \right] dg,$$

Precompute:

$$F(l + m, \rho, \hat{g}) := \int_{S^{d-1}} B_\sigma(\rho, \sigma \cdot \hat{g}) \left( e^{i\frac{\pi}{L}\rho\frac{1+e}{4}(l+m) \cdot (\hat{g} - \sigma)} - 1 \right) d\sigma,$$

And approximate:

$$G(l, m) \approx \sum_{\rho, \hat{g}} w_\rho w_{\hat{g}} \rho^{d-1} e^{-i\frac{\pi}{L}\rho m \cdot \hat{g}} F(l + m, \rho, \hat{g}),$$

## SEPARATE VS. FULL

For loss term:

$$G(m) := \int_{B_R} e^{-i\frac{\pi}{L}m \cdot g} \left[ \int_{S^{d-1}} B_\sigma(|g|, \sigma \cdot \hat{g}) \, d\sigma \right] \, dg,$$

Compute:

$$\hat{Q}_k^- = \sum_{\substack{l,m=-\frac{N}{2} \\ l+m=k}}^{\frac{N}{2}-1} \hat{f}_l \left( G(m) \hat{f}_m \right)$$

## COMPLEXITY

$$G(l, m) \approx \sum_{\rho, \hat{g}} w_\rho w_{\hat{g}} \rho^{d-1} e^{-i \frac{\pi}{L} \rho m \cdot \hat{g}} F(l + m, \rho, \hat{g}),$$

- $\rho$  direction:  $O(N)$
- $\hat{g}$  direction:  $M \ll N^2$  in 3D
- $N_p = O(MN)$
- Total:  $O(MN^{d+1} \log N)$

## 2D VHS MODEL

$$\begin{aligned}F(k,\rho,\hat{g}) &= \int_{S^1} C_\lambda \rho^\lambda \left( e^{i\frac{\pi}{L}\rho\frac{1+e}{4}k\cdot(\hat{g}-\sigma)} - 1 \right) \, d\sigma \\&= 2\pi C_\lambda \rho^\lambda \left[ e^{i\frac{\pi}{L}\rho\frac{1+e}{4}k\cdot\hat{g}} J_0\left(\frac{\pi}{L}\rho\frac{1+e}{4}|k|\right) - 1 \right],\end{aligned}$$

$$\hat{Q}_k \approx \sum_{\rho,\hat{g}} w_\rho w_{\hat{g}} \rho F(k,\rho,\hat{g}) \sum_{\substack{l,m=-\frac{N}{2} \\ l+m=k}}^{\frac{N}{2}-1} \hat{f}_l \left[ e^{-i\frac{\pi}{L}\rho m\cdot\hat{g}} \hat{f}_m \right],$$

$$\hat{Q}_k^- \approx \sum_{\substack{l,m=-\frac{N}{2} \\ l+m=k}}^{\frac{N}{2}-1} \hat{f}_l \left[ \sum_\rho w_\rho 4\pi^2 C_\lambda \rho^{\lambda+1} J_0\left(\frac{\pi}{L}\rho|m|\right) \hat{f}_m \right].$$

## 3D VHS MODEL

$$\begin{aligned}F(k,\rho,\hat{g}) &= \int_{S^2} C_\lambda \rho^\lambda \left( e^{i\frac{\pi}{L}\rho\frac{1+e}{4}k\cdot(\hat{g}-\sigma)} - 1 \right) \, d\sigma \\&= 4\pi C_\lambda \rho^\lambda \left[ e^{i\frac{\pi}{L}\rho\frac{1+e}{4}k\cdot\hat{g}} \operatorname{Sinc}\left(\frac{\pi}{L}\rho\frac{1+e}{4}|k|\right) - 1 \right],\end{aligned}$$

$$\hat{Q}_k \approx \sum_{\rho,\hat{g}} w_\rho w_{\hat{g}} \rho^2 F(k,\rho,\hat{g}) \sum_{\substack{l,m=-\frac{N}{2} \\ l+m=k}}^{\frac{N}{2}-1} \hat{f}_l \left[ e^{-i\frac{\pi}{L}\rho m\cdot\hat{g}} \hat{f}_m \right],$$

$$\hat{Q}_k^- \approx \sum_{\substack{l,m=-\frac{N}{2} \\ l+m=k}}^{\frac{N}{2}-1} \hat{f}_l \left[ \sum_\rho w_\rho 16\pi^2 C_\lambda \rho^{\lambda+2} \operatorname{Sinc}\left(\frac{\pi}{L}\rho|m|\right) \hat{f}_m \right].$$

## NUMERICAL TEST 2D

We first consider the isotropic initial condition:

$$f_0(v) = \frac{1}{2\pi K^2} \exp\left(-\frac{v^2}{2K}\right) \left(2K - 1 + \frac{1-K}{2K}v^2\right),$$

where  $K = 1 - \exp(-1/16)/2$ . One can easily check that  $\rho_0 = 1$ ,  $u_0 = 0$  and  $T_0 = 1$ .

We compare the difference of temperature  $|T_{\text{num}} - T_{\text{ref}}|$  at some given time  $t_{\text{final}}$ . The numerical  $T_{\text{num}}$  is obtained by taking the moments of the numerical solution  $f_{\text{num}}$ , computed by our fast spectral method. The reference  $T_{\text{ref}}$  is obtained using the exact formula

## NUMERICAL TEST 2D

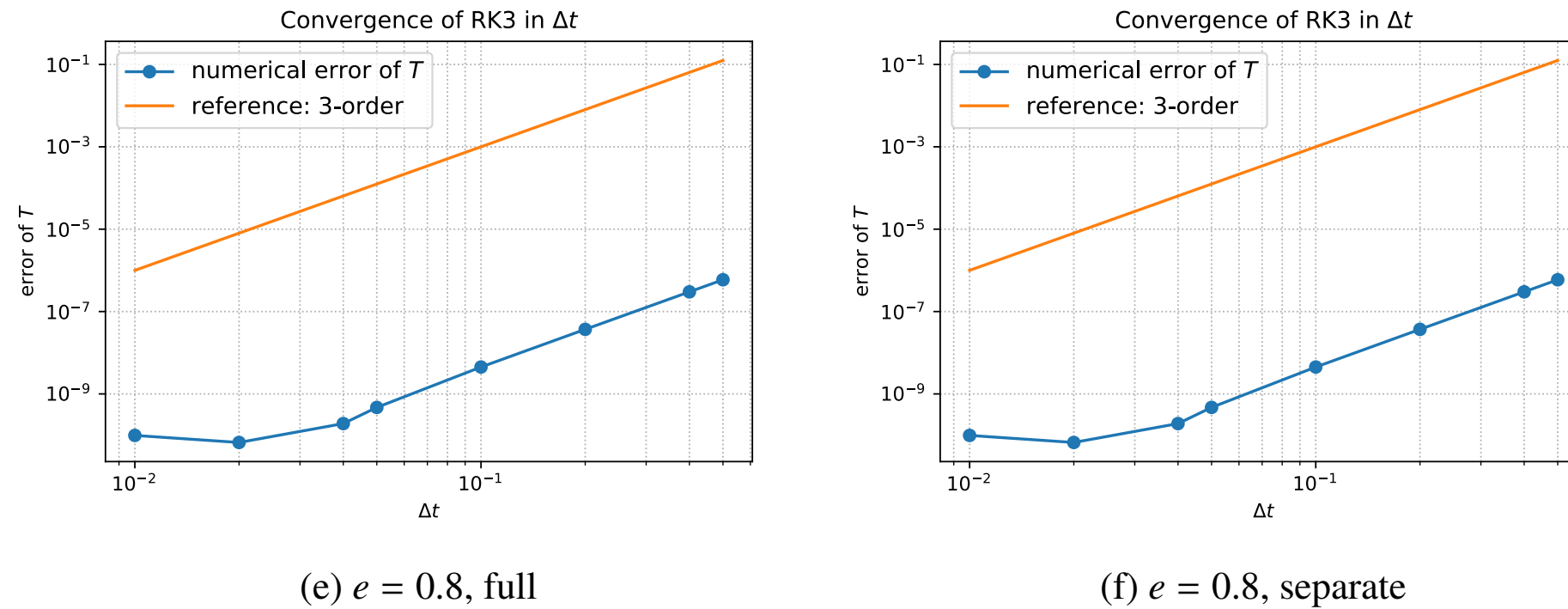
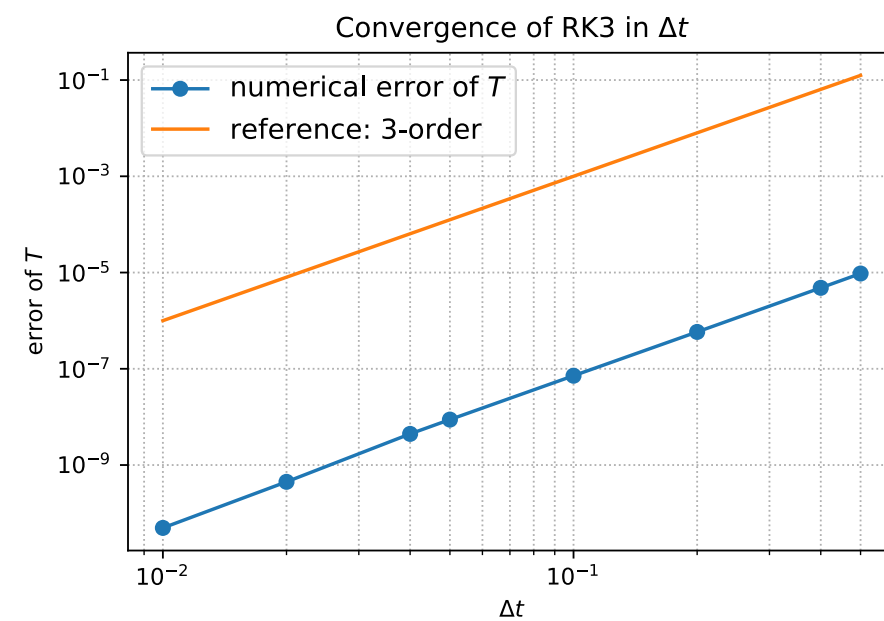
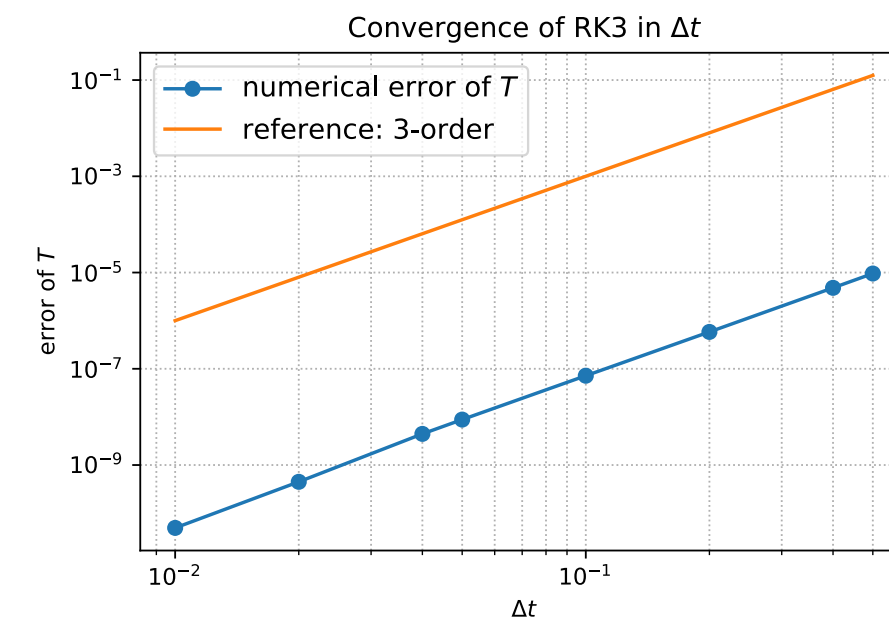


Figure 1: Convergence test in time of the 2D Maxwell molecule (isotropic solution) for  $e = 0.2, 0.5$  and  $0.8$ , and for both the “full” and “separate” methods. Errors shown here are  $|T_{\text{num}} - T_{\text{ref}}|$  at  $t_{\text{final}} = 2$ .  $N = 64$ ,  $N_\rho = 30$ ,  $M_{\text{cir}} = 30$ ,  $R = 7.8$ ,  $L = 8.61$ .

## NUMERICAL TEST 2D

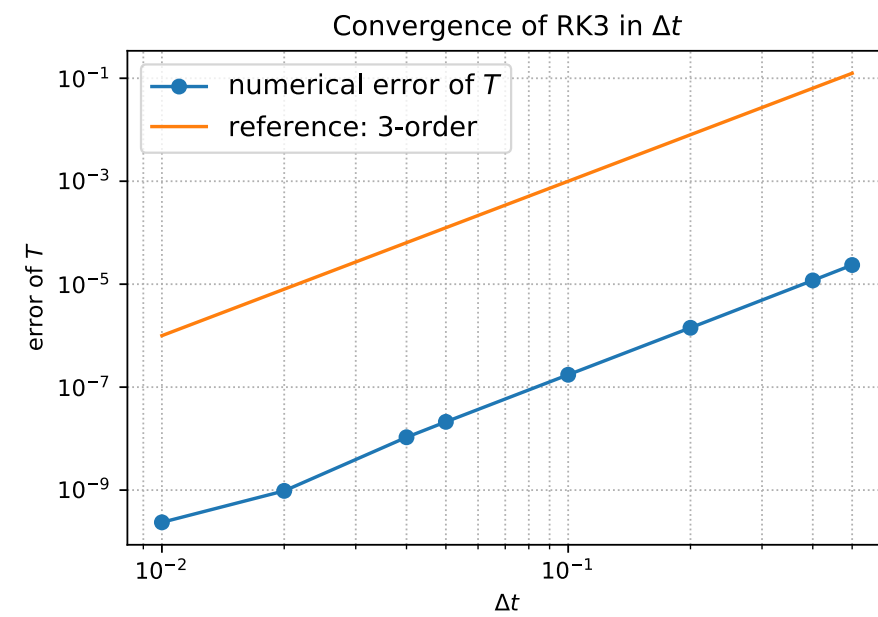


(c)  $e = 0.5$ , full

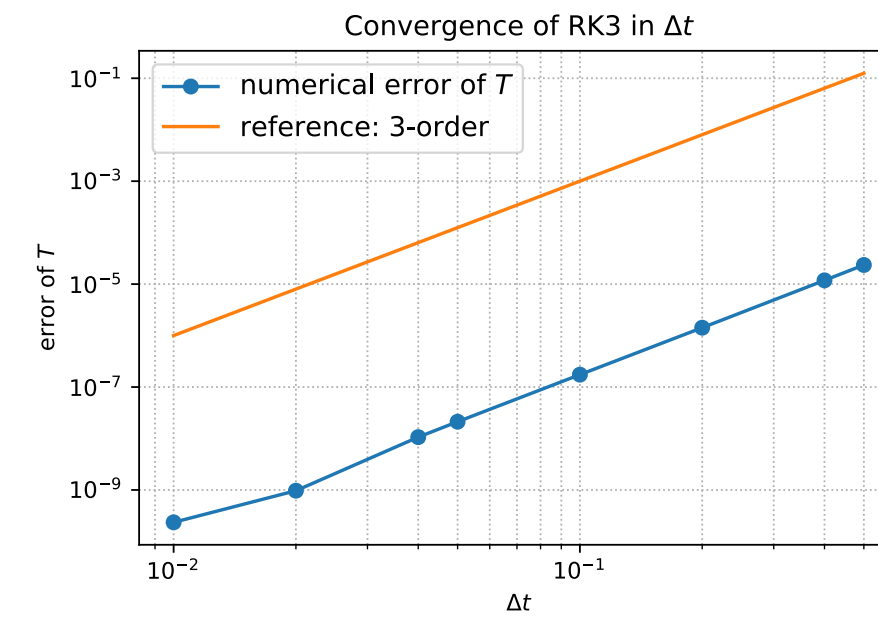


(d)  $e = 0.5$ , separate

## NUMERICAL TEST 2D



(a)  $e = 0.2$ , full



(b)  $e = 0.2$ , separate

## NUMERICAL TEST 2D

$N$	full	separate
8	5.52666966e-01	5.52666966e-01
16	4.88586534e-04	4.88821204e-04
32	1.13897201e-07	1.14430393e-07
64	9.82520731e-11	9.82359749e-11
128	1.00117470e-10	1.00099595e-10

(c)  $e = 0.8$

Table 1: Convergence test in  $N$  of the 2D Maxwell molecule (isotropic solution) for  $e = 0.2, 0.5$  and  $0.8$ , and for both the “full” and “separate” methods. Errors shown here are  $|T_{\text{num}} - T_{\text{ref}}|$  at  $t_{\text{final}} = 2$ .  $\Delta t = 0.01$ ,  $N_\rho = 30$ ,  $M_{\text{cir}} = 30$ ,  $R = 7.8$ ,  $L = 8.61$ .

## NUMERICAL TEST 2D

---

$N$	full	separate
8	7.98706096e-01	7.98706096e-01
16	6.42644165e-03	6.42641236e-03
32	4.55730861e-06	4.55713801e-06
64	4.93770580e-11	4.93595165e-11
128	3.14279713e-11	3.13873372e-11

---

(b)  $e = 0.5$

## NUMERICAL TEST 2D

$N$	full	separate
8	9.21116565e-01	9.21116565e-01
16	1.27640374e-02	1.27634481e-02
32	6.79745658e-06	6.79544555e-06
64	2.36438646e-10	2.34851361e-10
128	6.13890050e-11	6.30565600e-11

(a)  $e = 0.2$

## 3D INELASTIC MAXWELL MOLECULE

Consider the constant collision kernel  $B_\sigma = \frac{1}{4\pi}$  and the initial condition:

$$f_0(v) = \frac{1}{2(2\pi K)^{3/2}} \exp\left(-\frac{v^2}{2K}\right) \left( \frac{5K - 3}{K} + \frac{1 - K}{K^2} v^2 \right),$$

where  $K = 1 - \exp(-6.5/6)$ . Note that  $\rho_0 = 1$ ,  $u_0 = 0$  and  $T_0 = 1$ .

$M_{\text{sph}}$	$ T_{\text{num}} - T_{\text{ref}} $
6	0.0013957739849754791
12	9.9706271716293315e-05
32	2.2499901350947482e-06
48	2.4272557155313734e-06
70	2.4703481364962698e-06
94	2.4703481364962698e-06
120	2.453380453903975e-06

Table 3: Convergence test in  $M_{\text{sph}}$  of the 3D Maxwell molecule for  $e = 0.2$ . Errors shown here are  $|T_{\text{num}} - T_{\text{ref}}|$  at  $t_{\text{final}} = 1$ .  $\Delta t = 0.01$ ,  $N = 32$ ,  $N_\rho = 30$ ,  $R = 7$ ,  $L = 7.72$ .

## 3D INELASTIC MAXWELL MOLECULE

$M_{\text{sph}}$	$ Q_{\text{num}} - Q_{\text{direct}} _{L^\infty}$
6	0.00041820767783433107
12	3.1726851245650724e-05
32	6.5752814213618921e-07
48	5.6132233266191489e-07
70	2.6714628356683257e-07
94	1.0508293902503248e-07
120	2.8872928147741922e-08

Table 4: Convergence test in  $M_{\text{sph}}$  of the 3D Maxwell molecule for  $e = 0.2$ . Errors shown here are  $|Q_{\text{num}} - Q_{\text{direct}}|_{L^\infty}$  at  $t_{\text{final}} = 1$ .  $\Delta t = 0.01$ ,  $N = 32$ ,  $N_\rho = 30$ ,  $R = 7$ ,  $L = 7.72$ .

## 3D INELASTIC MAXWELL MOLECULE

$N$	direct	fast
8	32.3ms	17.6ms
16	602ms	140ms
32	23.7s	1.18s
64	—	9.7s

Table 5: Average running time per evaluation of the collision operator. Comparison between the direct method and the fast method for various  $N$  and fixed  $N_\rho = 30$ ,  $M_{\text{sph}} = 32$ .

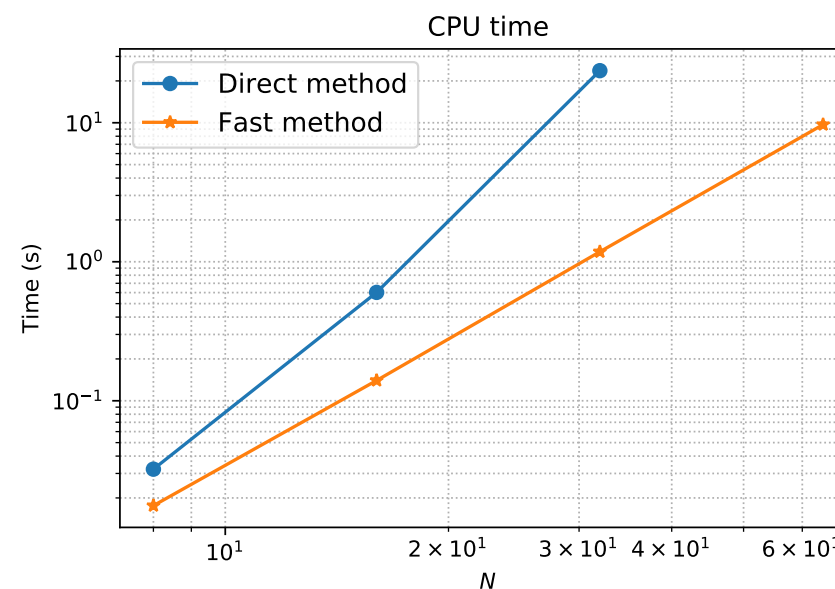


Figure 2: Same numbers as in Table 5 plotted in a log-log scale.

## Haff's cooling law

$$T(t) = \frac{T_0}{(1 + C_0 t)^2},$$

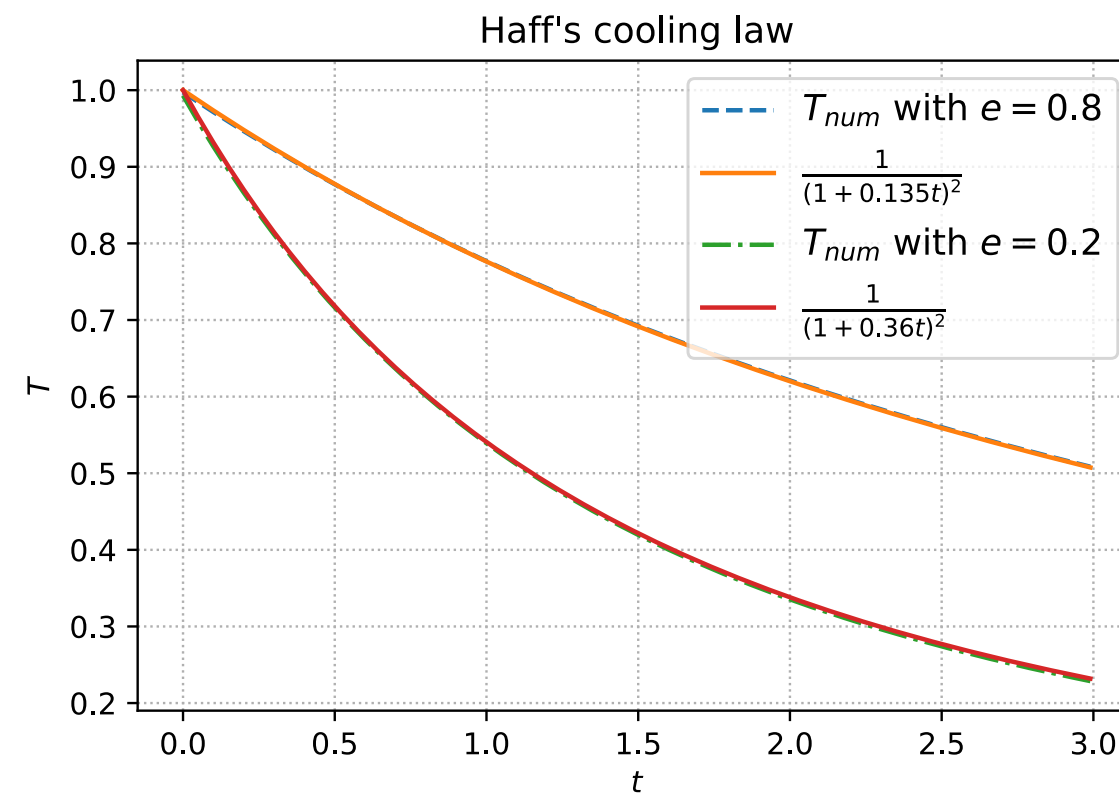


Figure 3: Haff's cooling law.  $\Delta t = 0.01$ ,  $N = 32$ ,  $N_\rho = 30$ ,  $M_{\text{sph}} = 32$ ,  $R = 7$ ,  $L = 7.72$ .

## CONCLUSION

- We introduced a simple strategy to accelerate the direct Fourier spectral method for the inelastic Boltzmann collision operator
- Reduce the computational complexity by orders of magnitude as well as relieve the memory bottleneck in the direct method
- In the future, we will apply the fast solver to the spatially inhomogeneous setting and to simulate more interesting problems in granular materials